

Design and FEM Analysis of Plastic Parts of a Tie-Rod Composite Hydraulic Cylinder

Marek LUBECKI*, **Michał STOSIAK***, **Mykola KARPENKO****, **Kamil URBANOWICZ*****, **Adam DEPTUŁA******, **Rafał CIEŚLICKI***

*Wrocław University of Science and Technology, Faculty of Mechanical Engineering, 7/9 Łukasiewicza St., 50-371 Wrocław, Poland, E-mails: marek.lubecki@pwr.edu.pl, michal.stosiak@pwr.edu.pl, rafal.cieslicki@pwr.edu.pl

**Vilnius Gediminas Technical University, Faculty of Transport Engineering, Saulėtekio al. 11, LT-10223 Vilnius, Lithuania, E-mail: mykola.karpenko@vlniustech.lt

***West Pomeranian University of Technology, Faculty of Mechanical Engineering and Mechatronics, 70-310 Szczecin, Polan., E-mail: kamil.urbanowicz@zut.edu.pl

****Opole University of Technology, Faculty of Production Engineering and Logistics, Opole University of Technology, 76 Prószkowska St., 45-758 Opole, Poland, E-mail: a.deptula@po.edu.pl

<https://doi.org/10.5755/j02.mech.31817>

1. Introduction

Hydrostatic drives are a type of machine drive that is widely used in many industries [1, 2]. This is due to a number of advantages, such as a high ratio of power transferred to the weight of the system, the possibility of easy control or the freedom of arrangement of elements on the machine. Many requirements are placed on hydraulic systems and the list is not closed. Some of the most important requirements for hydraulic systems and components include: reliable operation under the specified conditions, precision of movement, small dimensions, low weight, no dynamic excesses, high efficiency. Recently, the list of requirements has been extended to include environmentally friendly features.

Hydraulic receivers play a particularly responsible role in hydraulic systems, as they are directly affected by external loads and are subjected to highly variable operating conditions. In such systems, cylinders are actuators whose task is to convert the energy of the pressure of the liquid into the energy of the reciprocating movement of the piston [3].

Work is underway to reduce the size and weight of hydrostatic components [4] and systems. New rules for the design and operation of miniaturized systems, known as micro-hydraulic systems, are being developed [5]. Weight reduction can be done by using composite materials [6 – 8] or plastics [9 – 11] to manufacture some or all of the elements [12]. The search for the use of new materials for hydraulic cylinder cylinders continues unabated. Among the materials being researched for use in hydraulic cylinder cylinders are [13]: polypropylene (PP), polyamide (PA), polyoxymethylene (POM), Al-Zn alloy (Al 7075-T6) [14], spheroidal cast iron (60-40-18), low-carbon structural steel (BS970070M20) [15], Al 7075-T6 and a composite material consisting of 40% epoxy resin and 60% carbon fibres [16]. The use of new materials in the manufacture of hydraulic cylinders should not result in a deterioration of their operating characteristics such as operating pressures and temperatures. In addition, cylinders made from the new materials should be more resistant to external influences, e.g. moisture, salinity. Reducing the weight of hydraulic cylinders and other hydraulic components is of particular importance in mobile machinery or ships or aircraft. In mobile machines such as loaders, excavators, self-propelled mining machin-

es, agricultural machines, road machinery, construction machines, a reduction in the weight of the hydraulic components will result in a reduction in the power required to drive the machine in transients. Reducing the weight of ships or aircraft is particularly important. This will also result in changes to the dynamic characteristics of these machines considered as discrete multi-mass systems [17].

An important step is the correct process of cylinder design and computerised strength analysis. The paper presents the process of design and strength analysis using the finite element method of the base and gland of a tie-rod hydraulic cylinder. The elements were made of PET plastic. In order to implement a non-linear material model into the calculations, material tests were performed using a static tensile test in accordance with the ISO 527-2 standard [18].

2. Research object

The considered components are made of polyethylene terephthalate (PET) supplied by Ensinger Plastics under the trade name TECAPET. It is a plastic from the group of polyesters widely used for the production of fibers, packaging, machine parts as well as matrixes of composite materials. It is characterized by satisfactory mechanical properties and a high glass transition temperature (above 80°C). This is important because the temperature of the working fluid in hydraulic systems often reaches just around 80°C. The basic mechanical and thermal properties of the material declared by the manufacturer are shown in Table 1.

Table 1

Basic properties of the TECAPET material declared by the manufacturer

Parameter	Value
Young's modulus, MPa	3100
Ultimate tensile strength, MPa	79
Glass transition temperature, °C	81

In order to accurately determine the stress-strain relationship, which is highly nonlinear for plastics, a static tensile test was carried out in accordance with ISO 527-2. The resulting σ - ϵ curve implemented in the material model during the calculations is shown in Fig. 1. The model used in this case was the Multilinear Isotropic Hardening model.

The tensile strength experimentally determined low value of 75 MPa, and the strain at break is 5125 $\mu\text{m}/\text{m}$.

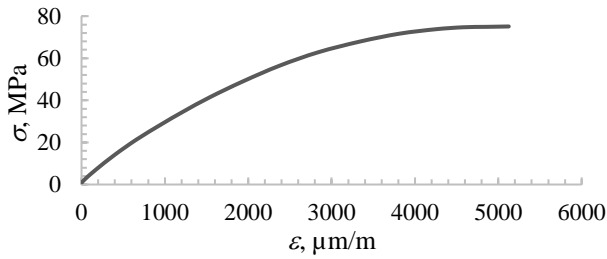
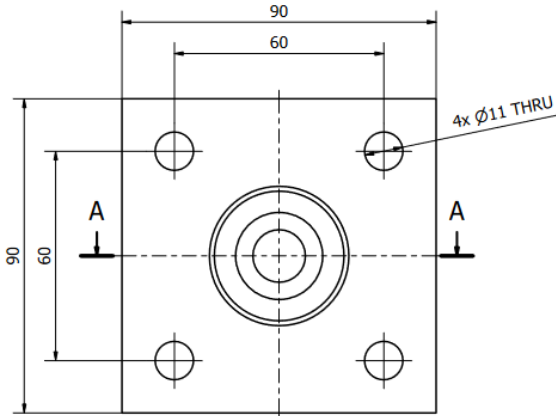


Fig. 1 Experimentally determined stress-strain curve for the TECAPET material by [11]



A-A (1 : 1)

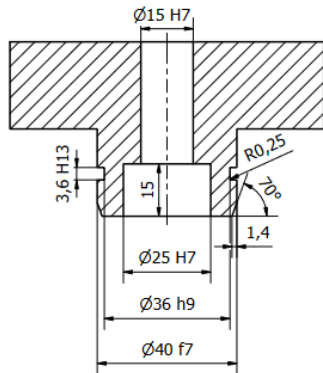


Fig. 2 Basic dimensions and shape of the base

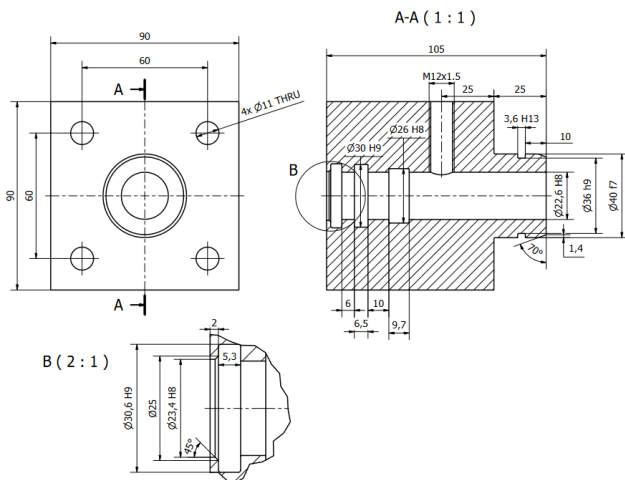


Fig. 3 Basic dimensions and shape of the gland

The subjects of the considerations were the base and the gland of the tie-rod hydraulic cylinder. The task of

the base is to seal one of the barrel ends and to supply the liquid to the piston chamber. The task of the gland, in addition to the static seal of the barrel and the supply of liquid to the piston rod chamber, is a movement seal on the surface of the piston rod and, together with an appropriately selected seal, ensuring a reciprocating movement with minimal friction losses. Both elements are connected with each other by means of four threaded tie-rods preventing movement along the axis of the cylinder. Drawings of the base and the gland are presented in Figs. 2 and 3, respectively.

3. FEM analysis and results

Strength calculations were carried out using the finite element method (FEM) in the ANSYS Mechanical 2021 software. The software license was granted by the Wrocławskie Centrum Sieciowo-Superkomputerowe. Fig. 4 shows the geometric model of the system. It consisted of a base with a connector, a gland with a connector, a barrel, tie-rods and washers. Due to the existing symmetry, 1/2 of the system was modeled.

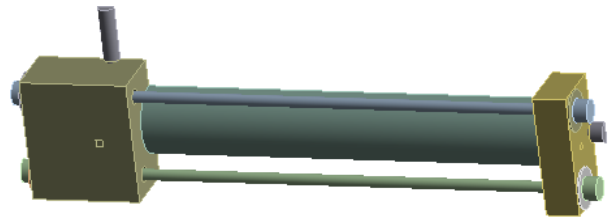


Fig. 4 Model of a geometry of a system

The model was divided into 3 mm finite elements for tie-rods, washers and connectors and 1 mm for the base, gland and barrel. The Hex20 type predominated among the finite elements. The final mesh had 762,218 nodes and 196,468 elements (Fig. 5).

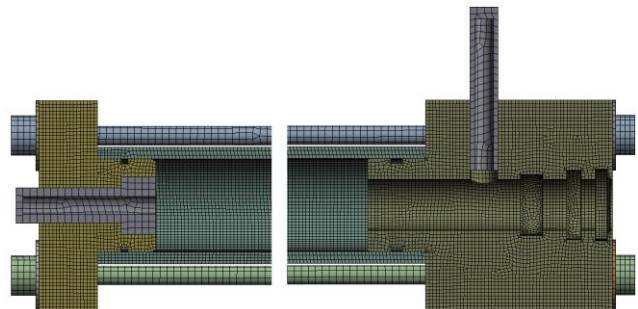


Fig. 5 Geometric model divided into finite elements

The base and the gland were assigned the experimentally determined nonlinear stress-strain relationship, the Poisson ratio of 0.33 and the density of 1.36 g/cm^3 . The connections, washers, tie-rods and the barrel were assigned the Structural Steel material from the ANSYS library ($E = 200 \text{ GPa}$, $\nu = 0.3$). Bonded contacts are provided between the washers and tie-rods, as well as between the connectors the base and the gland. A frictional contact with a friction coefficient of 0.2 was chosen between the washers and the plastic elements, as well as between the plastic elements and the barrel. The model was fixed in space by removing all degrees of freedom on the faces of the bolt heads from the base side (Fig. 6).

The simulation was performed in two steps. In the first step, the tie-rods were pre-tensioned with a force of

4900 N on each of the rod, which corresponded to tightening the nuts with a torque of 10 Nm (Fig. 7). In the second step, an internal pressure load of 20 MPa was added (Fig. 8).

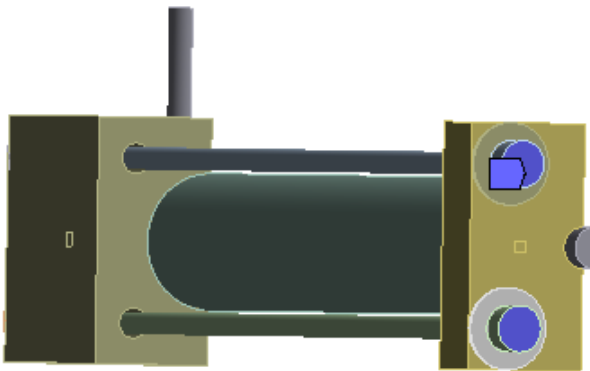


Fig. 6 The places of fixed constraints of the computational model

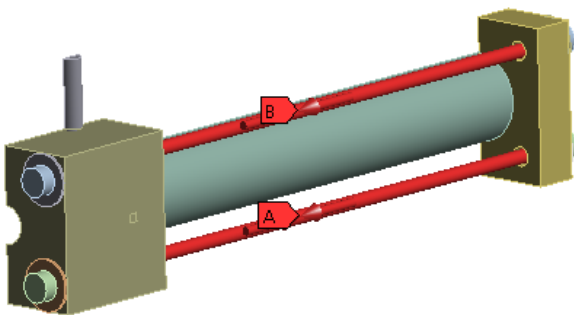


Fig. 7 Preloading the tie-rods in the first step of the simulation

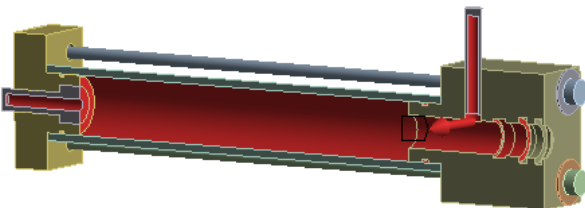


Fig. 8 Loading the model with internal pressure in the second step of the simulation

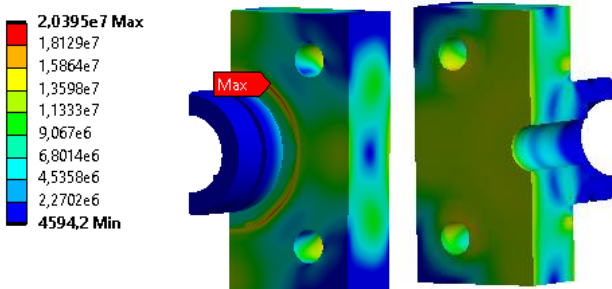


Fig. 9 Stress on the base's surface after initial tensioning of the tie-rods

In the Figs. 9 and 10 show the stresses reduced according to the Huber-Mises hypothesis on the surfaces of the elements after the initial tensioning of the tie-rods. The maximum stress for the base was 20.4 MPa and was in the region of contact with the outer edge of the cylinder, while for the gland it was 21.5 MPa and was at the transition from the face to cylindrical surface entering the barrel interior.

In the Figs. 11 and 12 show the reduced stresses on

the surfaces of the base and gland after loading the cylinder with internal pressure. The maximum stresses for the base were 29.8 MPa and were on the edge of the connector hole, while for the gland - less than 44 MPa and were on the edge between the piston rod hole and the connector hole.

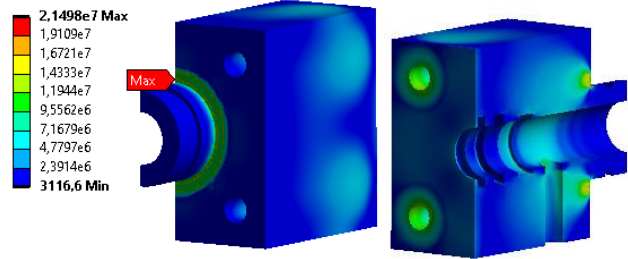


Fig. 10 Stress on the gland's surface after initial tensioning of the tie-rods

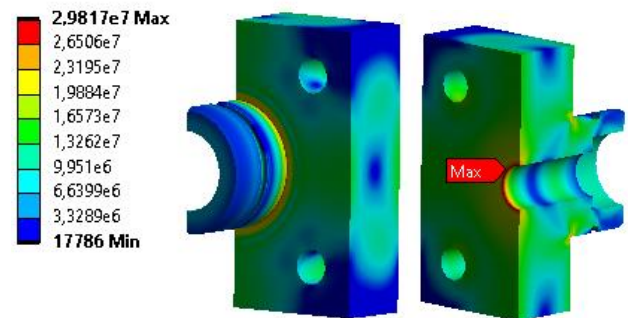


Fig. 11 Stress on the base's surface after loading with internal pressure

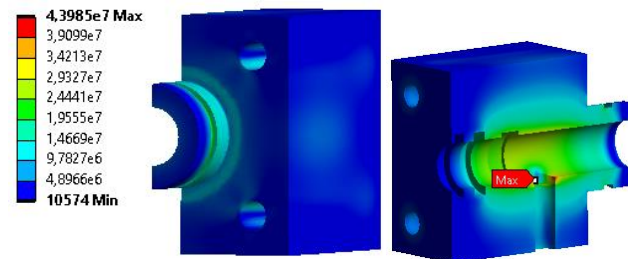


Fig. 12 Stress on the gland's surface after loading with internal pressure

4. Prototype test and results

The physical prototypes made from Tecapet White solid material produced by Ensinger Plastics. Measurements of the deformation were carried out using TENMEX TF 5 strain gauges with a gauge constant of $2.19 \pm 2\%$, and the resistance $350 \Omega \pm 2\%$. The HBM QuantumX MX440B interface and a PC with Catman AP software were used for the acquisition of measurement data. The arrangement of strain gauges on the base and gland is shown in Fig. 13.

Then, the elements were mounted in the cylinder and subjected to loads identical to those assumed in the FEM model (step 1 – pretension of the tie-rods, step 2 - loading with internal pressure of 20 MPa).

Tables 2 and 3 present the results of the FEM analysis and experimental measurements of the base and gland strain. The results obtained by means of FEM were read at the places where the strain gauges were attached to the prototypes and averaged over the surface of the measuring grid of the strain gauges.

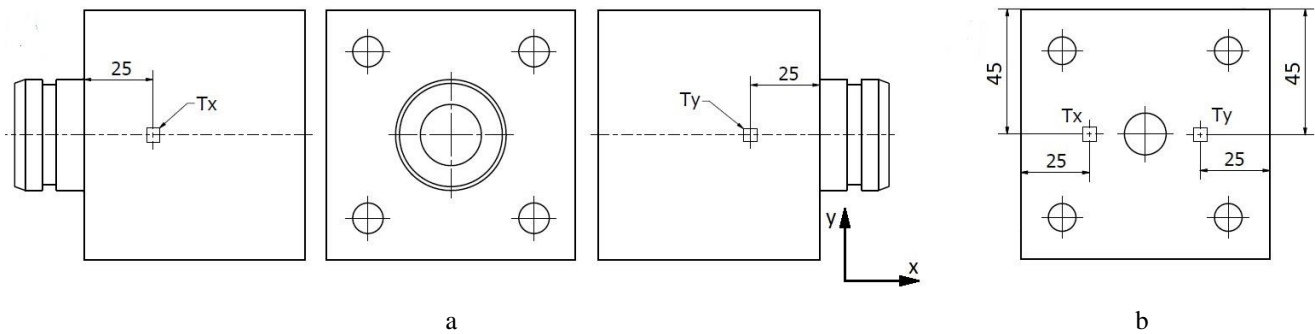


Fig. 13 Strain gauges placement on: a) gland, b) base

Table 2

Comparison of the results of the FEM analysis and experimental measurements of the base's deformation

	$\varepsilon_x, \mu\text{m/m}$			$\varepsilon_y, \mu\text{m/m}$		
	FEM	Exp.	Diff.	FEM	Exp.	Diff.
St.1	1321	931	42%	3186	3462	8%
St. 2	1130	909	24%	5106	5700	10%

Table 3

Comparison of the results of the FEM analysis and experimental measurements of the gland's deformation

	$\varepsilon_x, \mu\text{m/m}$			$\varepsilon_y, \mu\text{m/m}$		
	FEM	Exp.	Diff.	FEM	Exp.	Diff.
St. 1	-311	-300,7	4%	307	343,2	10%
St. 2	-101	-99,8	1%	1592	1335	19%

The greatest differences between the experiment and the calculations were noted for the strain ε_x of the base and amounted to 42% in the first step and 24% in the second step, respectively. These differences could result from inaccuracies in the mounting of the strain gauges as well as the uneven pretensioning of all four tie-rods of the prototype.

The analysis of the results revealed that in the places where the sensors were mounted, there was a significant variation in the strain values, and thus the inaccuracies in their positioning had a large impact on the measurement results.

4. Conclusions

The paper presents the process of analysis by the finite element method of the base and the gland of a tie-rod composite hydraulic cylinder. The analysis was carried out in two steps, taking into account the preload of the rods and the internal pressure load. Numerical calculations were experimentally validated by means of bench tests of the prototype with the use of strain gauges. The greatest differences between the experiment and the calculations were noted for the strain ε_y of the base and amounted to 42% in the first step and 24% in the second step, respectively. The obtained results were in agreement both qualitatively and quantitatively. The absolute differences between the experimental and calculated values were small in most cases. The analysis of the results revealed that in the places where the sensors were mounted, there was a significant variation in the strain values, and thus the inaccuracies in their positioning had a large impact on the measurement results. The maximum values of stresses in the FEM analysis were at the corners and places of changes in cross-sections, which could lead to the

formation of numerical singularities. The actual stress values at these points are probably slightly lower.

References

1. **Jaidev Vyas, J.; Gopalsamy, B.; Joshi, H.** 2018. Electro-Hydraulic Actuation Systems, Springer Briefs in Applied Sciences and Technology, 63 p.
2. **Stryczek, S.** 2005. Napęd Hydrostatyczny, WNT, Warszawa, 449 p. (In Polish). Available from Internet: <https://docer.pl/doc/xecevsv>.
3. **Salam, M.** 2022. Hydraulic Cylinders. In: Fundamentals of Pneumatics and Hydraulics, Springer, 124 p. https://doi.org/10.1007/978-981-19-0855-2_7.
4. **Rodionov, L.; Stryczek, J.; Rekadze, P.** 2021. Challenges in design process of gear micropump from plastics, Archives of Civil and Mechanical Engineering 21(34): 1-14. <https://doi.org/10.1007/s43452-020-00164-5>.
5. **Kollek, W.** 2011. Fundamentals of design, modelling and operation of microhydraulic components and systems, Publishing House of Wrocław University of Science and Technology, Wrocław (in Polish).
6. **Solazzi, L.; Buffoli, A.; Formicola, R.** 2020. The multi-parametric weight optimization of a hydraulic actuator, Actuators 9(3): 1-19. <https://doi.org/10.3390/act9030060>.
7. **Solazzi, L.** 2021. Stress variability in multilayer composite hydraulic cylinder, Composite Structures 259: 1-7. <https://doi.org/10.1016/j.compstruct.2020.113249>.
8. **Mantovani, S.** 2020. Feasibility analysis of a double-acting composite cylinder in high-pressure loading conditions for fluid power applications, Applied Sciences 10(3): 826. <https://doi.org/10.3390/app10030826>.
9. **Stryczek, J.; Banaś, M.; Krawczyk, J.; Marciniak, L.; Stryczek, P.** 2017. The fluid power elements and systems made of plastics, Procedia Engineering 176: 600-609. <https://doi.org/10.1016/j.proeng.2017.02.303>.
10. **Stryczek, P.; Przystupa, F.; Banas, M.** 2018. Research on series of hydraulic cylinders made of plastics, in 2018 Global Fluid Power Society PhD Symposium (GFPS), pp. 1-7. <https://doi.org/10.1109/GFPS.2018.8472385>.
11. **Lubecki, M.; Stosiak, M.; Gazińska, M.** 2021. Numerical and experimental analysis of the base of a composite hydraulic cylinder made of PET, in Lecture Notes in Mechanical Engineering 24: 396-405. https://doi.org/10.1007/978-3-030-59509-8_36.

12. **Skowrońska, J.; Zaczyński, J.; Kosucki, A.; Stawiński, L.** 2021. Modern materials and surface modification methods used in the manufacture of hydraulic actuators, in *Lecture Notes in Mechanical Engineering 24*: 427–439.
https://doi.org/10.1007/978-3-030-59509-8_39.
13. **Skowrońska, J.; Kosucki, A.; Stawiński, L.** 2021. Overview of materials used for the basic elements of hydraulic actuators and sealing systems and their surfaces modification methods, *Materials* 14: 1422.
<https://doi.org/10.3390/ma14061422>.
14. **Tubielewicz, K.; Turczyński, K.; Szygula, M.; Chlebek, D.; Michalczyk, H.** 2015. Hydraulic cylinder individual made light alloy, *Mechanik* 7: 907–912 (in Polish).
<https://doi.org/10.17814/mechanik.2015.7.311>.
15. **Luo, P.; Hi, J.; Tan, S.** 2018. Design and realization of hydraulic cylinder, *Region - Water Conservancy* 1(1): 27-34.
<https://doi.org/10.32629/rwc.v1i1.2>.
16. **Solazzi, L.; Buffoli, A.** 2019. Telescopic hydraulic cylinder made of composite material, *Applied Composite Materials* 26: 1189–1206.
<https://doi.org/10.1007/s10443-019-09772-8>.
17. **Harris Cyril, M.** 2009. *Harris' Shock and Vibration Handbook*, McGraw-Hill Education – Europe, 1456 p.
18. International Organization for Standardization, *Plastics — Determination of tensile properties — Part 2: Test conditions for moulding and extrusion plastics (ISO Standard 527-2:2012)*. 2011.

M. Lubecki, M. Stosiak, M. Karpenko, K. Urbanowicz, A. Deptuła, R. Cieśliski

DESIGN AND FEM ANALYSIS OF PLASTIC PARTS OF A TIE-ROD COMPOSITE HYDRAULIC CYLINDER

S u m m a r y

Due to a number of advantages, such as a high ratio of power transmitted to the weight of the system, the possibility of easy control and the freedom to arrange system elements on the machine, hydrostatic drive is one of the most popular methods of machine drive. The executive elements in such a system are hydraulic cylinders that convert the energy of the pressure of the liquid into the mechanical energy of the reciprocating motion. One of the disadvantages of conventional actuators is their weight, so research is being done to make them as light as possible. The directions of this research include the use of modern engineering materials such as composites and plastics.

The paper presents the process of designing, FEM analysis and experimental validation of the base and gland of a composite hydraulic cylinder. The considered elements are made of PET plastic. During the analysis, material non-linearity was taken into account, and the analysis itself was carried out in two steps. The first was the preloading of the tie-rods, and the second was the loading of the cylinder with internal pressure. The numerical calculations were experimentally validated by prototype tests with the use of strain gauges.

Keywords: hydraulic cylinder, plastic materials, FEM analysis, prototype test, strain, stress.

Received July 12, 2022

Accepted October 9, 2023



This article is an Open Access article distributed under the terms and conditions of the Creative Commons Attribution 4.0 (CC BY 4.0) License (<http://creativecommons.org/licenses/by/4.0/>).